Journal of Materials Chemistry C

PAPER

View Article Online
View Journal | View Issue

Cite this: J. Mater. Chem. C, 2018, 6, 12422

Synthesis and characterization of novel electrochromic devices derived from redox-active polyamide–TiO_2 hybrids†

Bo-Cheng Pan,‡[a] Wei-Hao Chen,‡[a] Tzong-Ming Lee[b] and Guey-Sheng Liou *[ac]

Received 4th September 2018,
Accepted 18th October 2018

DOI: 10.1039/c8tc04469d

rsc.li/materials-c

Two novel electrochromic (EC) polyamides with functional hydroxyl groups were successfully synthesized for preparing homogeneous hybrid films. The hydroxyl groups in the repeating units of the polymer backbones could serve as active sites in the sol–gel reaction to obtain organic–inorganic nanocomposites comprising titanium dioxide (TiO_2) and anodic EC polyamides (**TPPA-OH PA** and **TPB-OH PA**). By using the facile approach of an electron donor–acceptor hybrid system in this report, the EC response capability could be essentially enhanced during the colouring and bleaching process. In addition, the colouring contrast and electrochemical stability of the fabricated EC devices could be further increased by judiciously combining the complementary EC material of heptyl viologen (HV) and TiO_2.

Introduction

Electrochromism is the phenomenon whereby materials exhibit a reversible colour change in transmittance or absorption during electrochemical reduction or oxidation procedures. Electrochromic (EC) materials have been studied for decades, and various representative materials have been reported such as inorganic coordinating complexes (*e.g.*, Prussian blue[1] and Terpyridine complexes[2]), transition metal oxides (*e.g.*, WO_3[3]), conjugated polymers (*e.g.*, polyaniline[4]) and organic molecules (*e.g.*, viologen[5]). Inorganic EC materials are well known for their excellent switching stability, while organic EC materials have advantages such as high coloration efficiency, multiple colouring within the same material, and competitive processability. Generally, EC materials have mainly been investigated towards achieving colour changes in the visible light region (*e.g.*, 400–800 nm), and this gave rise to some typical products like optical switching devices, e-paper, camouflage materials, and smart windows.[6] Since 2002, our group has published reports on novel triphenylamine (TPA)-containing EC polymers that show interesting multicolour transitions and unique EC behaviours both in the visible and near infrared (NIR) regions.[7] Recently, panchromatic electrochromic devices (ECDs) with high optical contrast have also been successfully prepared;[8] however, the EC switching response capability and stability remain a challenge. Thus, the crucial issue is how to reduce the response time without sacrificing other EC properties, and the incorporation of a charge-acceptor metal oxide as a charge storage unit into EC polymers to produce polymer hybrid EC materials is one of the most efficient approaches for EC applications.

Polymer hybrids with strong covalent bonds between metal oxide and polymers have been studied in our group by designing and synthesizing various polymers with reactive functional groups (–OH and –COOH).[9] The sol–gel reaction is a convenient and effective method to combine the organic and inorganic materials that are used in transistor and resistor type memory devices.[10] TiO_2 is an excellent semi-conducting material that has been used in photo-catalysis,[11] solar cells,[12] EC devices, *etc.*[13] because TiO_2-based hybrid films demonstrate rapid charge transport properties and easy formation of nanostructures with large surface area. EC materials based on conducting polymers/TiO_2 hybrids have been prepared and investigated, but most of them work just by physical interaction between the two materials.[14] Consequently, replacing with strong covalent bonds within the hybrids could enable a more direct and effective process for the enhancement of EC properties.[15] According to the electrochromism principle, electron-withdrawing TiO_2 nanoparticles play an important role as an electron-storage counterpart in the ambipolar system during the EC process. The colour can be generated by the oxidation or reduction reaction, and the charges produced can be stored by TiO_2 within the donor–acceptor system.

[a] Institute of Polymer Science and Engineering, National Taiwan University, 10607, Taipei, Taiwan. E-mail: gsliou@ntu.edu.tw
[b] Material and Chemical Research Laboratories, Industrial Technology Research Institute, 195 Chung Hsing Road, 4th Sec., Hsinchu 31040, Taiwan
[c] Advanced Research Center for Green Materials Science and Technology, National Taiwan University, 10607, Taipei, Taiwan

† Electronic supplementary information (ESI) available: Experimental section, thermal properties, inherent viscosity and molecular weights of polyamides and supplementary EC behavior of films and ECDs derived from the polyamides and their hybrids. See DOI: 10.1039/c8tc04469d

‡ These authors contributed equally to this work.

Thus, in this report, we try to utilize TPA-based polyamides, typically anodic EC materials, to prepare novel redox-active polyamide–TiO_2 hybrids *via* the sol–gel reaction for studying the donor–acceptor effect on the EC performance. The results demonstrate that the EC response capability could be substantially enhanced during the colouring and bleaching process. In addition, the on/off optical contrast and electrochemical stability of the fabricated EC devices (ECDs) could be further increased by judiciously combining the complementary EC material of heptyl viologen (HV) and TiO_2 because the TPA-based EC polyamides could more effectively release and obtain electrons during oxidation redox switching *via* the covalent-bonded strong electron withdrawing TiO_2 near the polyamides.

Experimental

Materials

N,*N*′-bis(4-aminophenyl)-*N*,*N*′-di(4-methoxyphenyl)-4,4′-biphenyldiamine (**TPB**) and *N*,*N*′-bis(4-aminophenyl)-*N*,*N*′-di(methoxyphenyl)-1,4-phenylenediamine (**TPPA**) were synthesized based on previous reports.[16,17] Commercially available DL-2-hydroxysuccinic acid (ACROS), *N*,*N*-dimethylacetamide (DMAc) (TEDIA), pyridine (Py) (ACROS), triphenyl phosphite (TPP) (ACROS) and other reagents were used as received. The cathodic EC material, heptyl viologen tetrafluoroborate $HV(BF_4)_2$, was prepared as follows:[18] 4,4′-dipyridyl (3.12 g, 20 mmol) and 1-bromoheptane (31.4 mL, 200 mmol) were added into 30 mL of acetonitrile and refluxed for 6 h, the precipitate was filtered off after cooling down to room temperature and washed with organic solvents such as hot chloroform, acetone, hexane, and then dried in a vacuum to obtain a 96% yield of yellow powder, $HVBr_2$ (9.85 g). Afterwards, a solution of $HVBr_2$ (5.00 g) in DI water (50.0 mL) was dropwise added to a saturated solution of $NaBF_4$ (50.0 mL). After 30 min, the white solid $HV(BF_4)_2$ was obtained after filtration, which was then purified by recrystallization from ethanol.

Preparation of the TPPA-OH and TPB-OH polyamides (PAs)

Two diamine monomers, **TPPA** and **TPB**, were respectively used to synthesize the novel hydroxyl-containing polyamides, **TPPA-OH** and **TPB-OH**, with DL-2-hydroxysuccinic acid by direct polycondensation[19] as shown in Scheme 1. **TPPA-OH** as a typical example was prepared as follows: 502.6 mg (1.0 mmol) of the diamine monomer **TPPA**, 134.1 mg (1.0 mmol) of DL-2-hydroxysuccinic acid, 0.2 g of $CaCl_2$, 0.5 mL of TPP, 0.5 mL of Py, and 2.0 mL of NMP were heated under stirring at 60.0 °C for 12 h. After cooling down to room temperature, the polymer solution was poured slowly into 400 mL of a vigorously stirred methanol and water mixture (volume = 3 : 1), giving rise to a fiber-like precipitate that was then collected by filtration. After purification by Soxhlet extraction under reflux with water and methanol for 12 h, it was then dried under vacuum at 100 °C.

Preparation of TPPA-PATiX and TPB-PATiX hybrid films

In this paper, different weight percentages of TiO_2 were added to the polymer films for comparison. Therefore, **TPPA-PATiX** and **TPB-PATiX** were used to represent the EC hybrid films with different contents of TiO_2, where **X** is the wt% value of TiO_2. The preparation of the hybrid films is depicted in Scheme 1. **TPPA-PATi20** and **TPB-PATi20** are chosen as examples to describe the general synthesis route of the hybrid films as follows. Firstly, 20 mg of **TPPA-OH** or **TPB-OH** was dissolved in 10 mL of DMAc, and 0.04 mL of hydrochloric acid (36.5 v%) was added slowly into the polyamide (PA) solution and then stirred vigorously at room temperature for 30 min. After that, 0.021 mL (0.062 mmol) of $Ti(OBu)_4$ dissolved in 0.063 mL of butanol was added dropwise into the above solution using a syringe and then stirred at room temperature for 1.5 h. Afterwards, the resulting precursor solution was filtered through a 0.22 mm PTFE filter. Finally, the above precursor solution was cast onto the ITO-coated glass followed by a subsequent heating program at 40 °C for 4 h, 100 °C for 2 h, and then 160 °C for 2 h under vacuum to obtain the EC hybrid films with a thickness of around 300 ± 30 nm. After being characterized, the hybrid films were fabricated into electrochromic devices (ECDs) with the cathodic material, heptyl viologen (HV), introduced. The ECDs with different hybrid films were represented as **TPPA-PATiX/HV** and **TPB-PATiX/HV**.

Results and discussion

Polymer synthesis

Polyamides can generally be synthesized from dicarboxylic acid and diamine by direct polymerization at temperatures of 100–110 °C for about 3–6 hours.[16] However, the above reaction temperature was not appropriate for this work because DL-2-hydroxysuccinic acid possesses a functional hydroxyl group that could also react with the carboxylic group at higher temperature, resulting in a cross-linking structure during the polymerization procedure. Consequently, the modified reaction conditions with a lower temperature (60 °C) and longer reaction time (12 h) were adopted. The FT-IR spectra of the obtained PAs only exhibited the characteristic absorption peaks of the amide functional group at 1670 cm^{-1} without an ester absorption peak in the range of 1735–1750 cm^{-1} (as shown in Fig. 1). Thus, the hydroxyl group in DL-2-hydroxysuccinic acid was confirmed not to participate in the polymerization.

Basic properties of the PAs

The basic properties of the resulting two new PAs, **TPPA-OH** and **TPB-OH**, such as inherent viscosity, molecular weight, and solubility behaviour, are summarized in Tables S1 and S2 (ESI†). These PAs could dissolve in various organic solvents and their excellent solubility demonstrates that these PA films could be easily fabricated for practical application by solution casting. Furthermore, the thermal properties of the PAs were investigated by DSC and TGA (Fig. S1, ESI†), and the data are summarized in Table S3 (ESI†). These partially aromatic PAs also revealed high thermal stability without significant weight loss up to 300 °C both in nitrogen and air atmospheres with the glass-transition temperatures (T_gs) in the region of 180–195 °C.

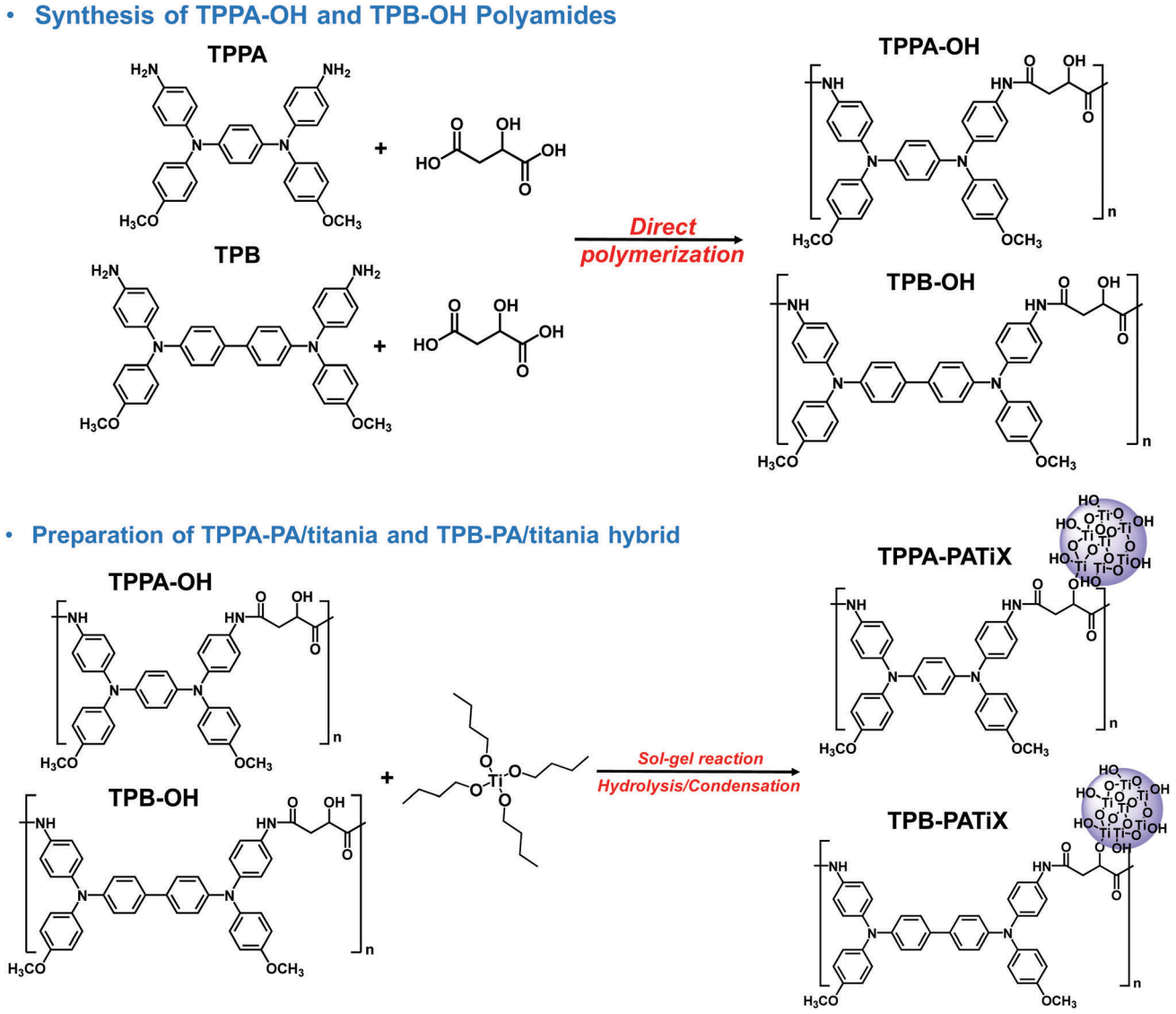

Scheme 1 Synthesis of the polyamides and their corresponding titania hybrids.

Synthesis and characterization of the PA hybrids

The compositions of the **TPPA-PATiX** and **TPB-PATiX** hybrid films prepared by the sol–gel reaction of the corresponding **TPPA-OH** and **TPB-OH** with titania precursors, respectively, are summarized in Table S4 (ESI†). The hydroxyl groups in these PA backbones could provide reaction sites for organic–inorganic bonding, resulting in homogeneous and transparent hybrid films with a well-dispersed titania domain size of less than 10 nm, as shown in Fig. 2. The excellent thermal stability of the obtained **TPPA-PATiX** and **TPB-PATiX** hybrid films was proved by TGA, and the char yield increased with the increasing titania content, as depicted in Fig. S2 (ESI†). Meanwhile, the TGA measurements under air flow could not only identify the thermal stability but also confirm the inorganic contents in the PA hybrid films by char yields that could be used to demonstrate the successful incorporation of the inorganic nanoparticles into the PAs.

Electrochemical properties of the EC materials

Typical cyclic voltammetry (CV) diagrams of the PAs and their related hybrid films coated on the ITO-coated glass substrates (thickness: 300 ± 50 nm; coated area: 25 mm × 6 mm) were measured in 0.1 M $TBABF_4$/PC at a scan rate of 50 mV s^{-1}, and the results are summarized in Fig. S3 (ESI†) for comparison. **TPPA-OH** and its hybrids all displayed two obvious oxidation redox peaks, implying that electrons could be removed from the two electroactive nitrogen sites, respectively, with a significant difference of applied voltage (ΔE), while **TPB-OH** only exhibited one broad redox peak comprising the first and second oxidation stages. Meanwhile, these PA hybrid EC materials, the **TPPA-PATiX** and **TPB-PATiX** hybrid films, both showed a lower oxidation potential than their corresponding pristine PAs, and the improvement could be enhanced obviously by increasing the amount of inorganic titania up to 20 wt%, as illustrated in Fig. S3 (ESI†). These EC hybrid films could be oxidized at a

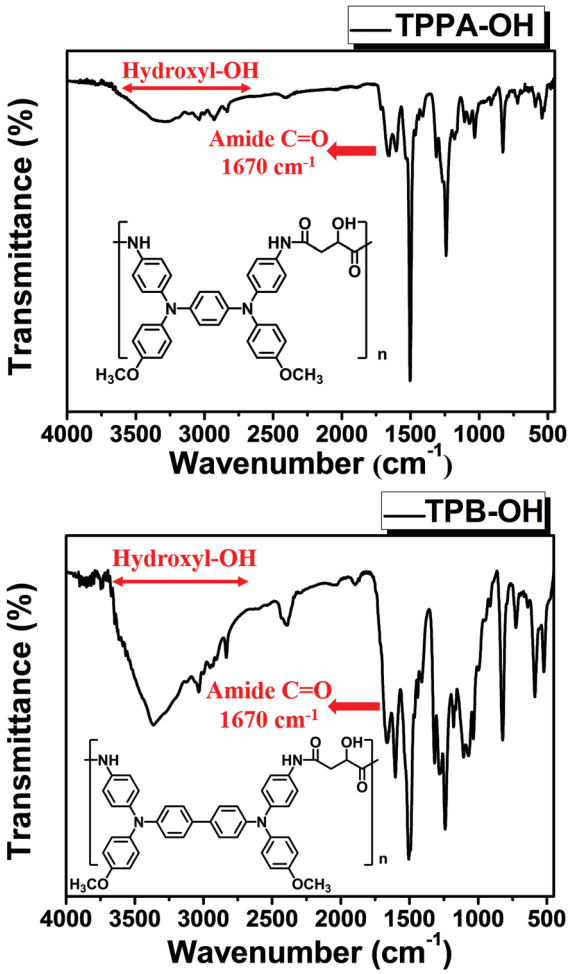

Fig. 1 FT-IR spectra of the PAs, **TPPA-OH** and **TPB-OH**.

lower driving voltage, implying that the enhancement of EC stability could be expected by this facile approach. Although these new EC PAs both have two oxidation states at the related applied voltages, the first oxidation state should be most valuable for application because of the lower driving energy and the higher EC stability. Therefore, the electrochemical stability of **TPPA-OH** and its hybrid films with different contents of titania was investigated at the first oxidation state, and the results are depicted in Fig. 3 and Table S5 (ESI†). Comparing with **TPPA-PATiX** over 1000 redox cycles, the pristine **TPPA-OH** exhibited the largest ΔE ($E_{pa} - E_{pc}$), indicating that the response capability for EC switching and bleaching during the oxidation

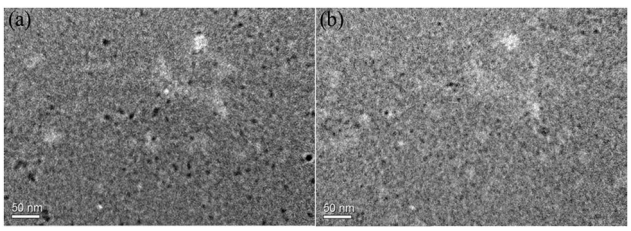

Fig. 2 TEM images of the hybrid materials (a) **TPPA-PATi20** and (b) **TPB-PATi20**.

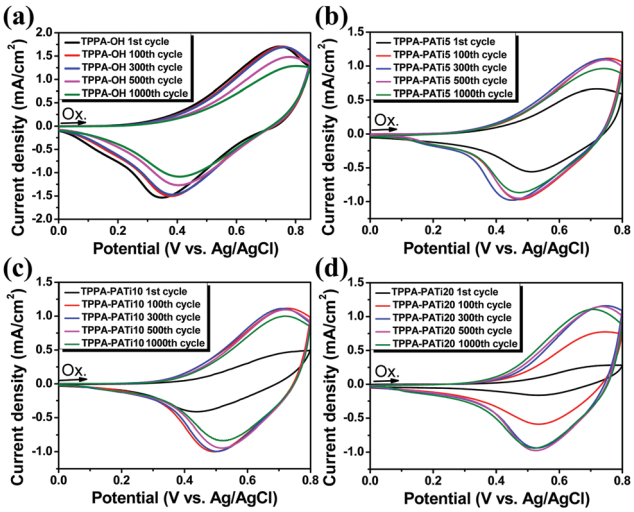

Fig. 3 Cyclic voltammetry diagrams of the 1st oxidation state stability test: (a) **TPPA-OH,** (b) **TPPA-PATi5,** (c) **TPPA-PATi10, and** (d) **TPPA-PATi20** on the ITO-coated glass substrate (coated area: 2.5 cm × 0.6 cm; thickness: 300 ± 50 nm) in 0.1 M $TBABF_4$/PC at a scan rate of 50 mV s^{-1}.

process was worse and slower than the hybrid system. In contrast, there was no obvious oxidation peak in the beginning few cycles for **TPPA-PATiX,** as shown in the CV diagrams, while the electrolyte can gradually diffuse into the hybrid films after hundreds of scans and the oxidation peak becomes clear. Besides, an enhancement of EC reversibility and stability for the hybrid system could also be observed over 1000 cycle scans in comparison to the pristine PA (Fig. 3). Furthermore, the EC response capability between switching and bleaching during the oxidation redox process for the hybrid system displayed smaller values of ΔE ($E_{pa} - E_{pc}$), and could be reduced from 0.38 V for **TPPA-OH** to 0.20 V and 0.17 V for **TPPA-PATi10** and **TPPA-PATi20** after 1000 cyclic scanning times, respectively (Table S5, ESI†), indicating that the response time could be effectively reduced for both switching and bleaching during the electrochemical and EC redox processes. However, the cross-linking degree of the hybrid films increased with increasing the content of titania, which could also hinder the diffusion of electrolyte into the EC hybrid film, thus the content of TiO_2 was limited to 20 wt% within this study.

Electrochemical behaviors of the electrochromic devices (ECDs)

The electrochemical properties and operation parameters such as driving potential of the ECDs were investigated. The respective CV diagrams for the devices derived from these PAs and their hybrids are depicted in Fig. S4 (ESI†). The oxidation potentials at the first stage that are needed to generate a cationic radical of the triarylamine moieties from the neutral state in a gel electrolyte system for the ECDs with a size of 20 mm × 20 mm derived from the pristine PAs of **TPPA-OH** and **TPB-OH** were 1.85 V and 2.1 V, respectively. In order to ameliorate the presence of defects owing to the gel type ECDs, a facile approach is just to incorporate TiO_2 into the redox-active

PAs *via* the sol–gel reaction and introduce the cathodic EC material HV into the gel electrolyte layer of the ECDs to solve this problem. The representative CV diagrams of the **TPPA-PATiX** and **TPB-PATiX** ECDs are also depicted in Fig. S4 (ESI†); the first oxidation potential could be gradually decreased from **TPPA-OH**: 1.85 V to **TPPA-PATi5**: 1.75 V, **TPPA-PATi10**: 1.63 V, and then **TPPA-PATi20**: 1.53 V. The **TPB-OH** hybrids also exhibited a similar tendency to the **TPPA-OH** hybrids, and the driving voltage decreased from 2.00 V to **TPB-PATi20**: 1.85 V because TiO_2 could accept the electrons from the PA moieties, making it easier for the electroactive TPA unit to lose an electron during the oxidation process and then for $TPA^{+\bullet}$ to gain an electron during the reduction process. Meanwhile, HV reveals a similar working principle in the ECDs, and it can effectively decrease the first oxidation potential to 1.05–1.10 V for **TPPA-OH/HV** and 1.35 V for **TPB-OH/HV**, as shown in Fig. S5 (ESI†). Consequently, by combining these two additional effects, the resulting ECDs with the lowest oxidation potential could be achieved for the **TPPA-PATi20/HV**: 0.98 V (**TPPA-PATi5**: 1.05 V and **TPPA-PATi10**: 1.02) and **TPB-PATi20/HV**: 1.25 V, as illustrated in Fig. 4.

Spectroelectrochemistry

Spectroelectrochemical measurements were performed to evaluate the optical behaviour of these PAs during the oxidation redox process. The characteristic absorption patterns of these two EC polymer films correlated to the applied potentials are depicted in Fig. S6 (ESI†). All the electroactive PAs are highly transparent and colourless at the neutral state (0.0 V). During oxidation (increasing applied voltage), the characteristic absorption in the visible light region could be greatly enhanced with peaks at a specific wavelength for each PA; for example, the **TPPA-OH** film showed new peaks at around 435 nm and 600 nm in the visible region, associated with an intense green colour owing to the structural change from PA to PA^{1+}. With the potential increasing to the second oxidation state to form PA^{2+}, a new broad band with a peak at around 835 nm and the colour changing from green to blue could be observed. Similarly, **TPB-OH** was also colourless at the neutral state (0 V) and exhibited two different colour forms related to the oxidation stages. The first oxidative form of PA^{1+} revealed a strong absorption peak at 500 nm with a reddish colour; then, **TPB**-based PA^{2+} generated in the second oxidation stage displayed a new broad band with a peak at around 954 nm accompanying the colour change from red to blue. The difference between these two chromogenic moieties was mainly attributed to the longer conjugation length of the biphenyl unit of **TPB-OH** compared to the phenyl unit of **TPPA-OH**, resulting in red-shifted absorption for **TPB-OH**. Furthermore, a series of ECDs was prepared from the two PAs (**TPPA-OH** and **TPB-OH**) and their corresponding ambipolar system combining the PAs and HV (**TPPA-OH/HV** and **TPB-OH/HV**), respectively, and its spectroelectrochemical behaviours were also studied and are summarized in Fig. S7 (ESI†).

Response behavior of electrochromic switching

The electrochromic switching of the devices with the ambipolar EC materials was studied to evaluate the transmittance changes of the characteristic absorption as a function of time and to obtain the response time by stepping potential repeatedly between the neutral and coloured states. The response time was determined as the time at 90% of the full switch in transmittance because it is difficult to perceive any further colour change beyond this point with the naked eye. As depicted in Fig. 5 and Fig. S8 (ESI†), the ECDs derived from **TPPA-OH/HV** exhibited a switching time of 8.0 s at 1.1 V for the colouring process at 435 nm and 30.5 s at −1.15 V for the bleaching process; the device based on **TPPA-PATi5/HV** showed a switching time of 5.2 s for colouring at 1.05 V and 22.5 s for bleaching at −1.1 V; the device based on **TPPA-PATi10/HV** showed a switching time of 5.0 s for colouring at 1.0 V and 18.0 s for bleaching at −1.05 V, and device based on **TPPA-PATi20/HV** showed a switching time of 5.0 s for colouring at 1.0 V and 17 s for bleaching at −1.05 V, respectively. In addition, the devices derived from **TPB-OH/HV** and **TPB-PATi20/HV** showed a similar tendency. According to these results, it is noteworthy that

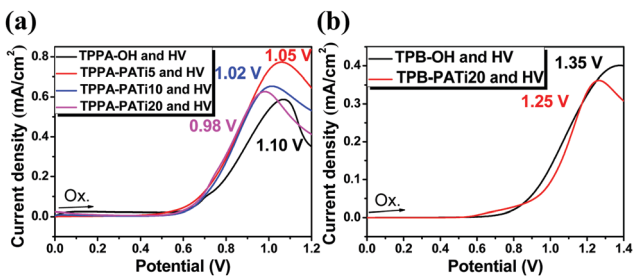

Fig. 4 Partial magnification of the cyclic voltammetry diagrams of (a) **TPPA-OH** and **TPPA-PATiX** hybrids, and (b) **TPB-OH** and **TPB-PATiX** hybrids (thickness: 300 ± 50 nm on the ITO-coated glass substrate (coated area: 2 cm × 2 cm) in 0.1 M TBABF4/PC electrolyte with 0.015 M HV.

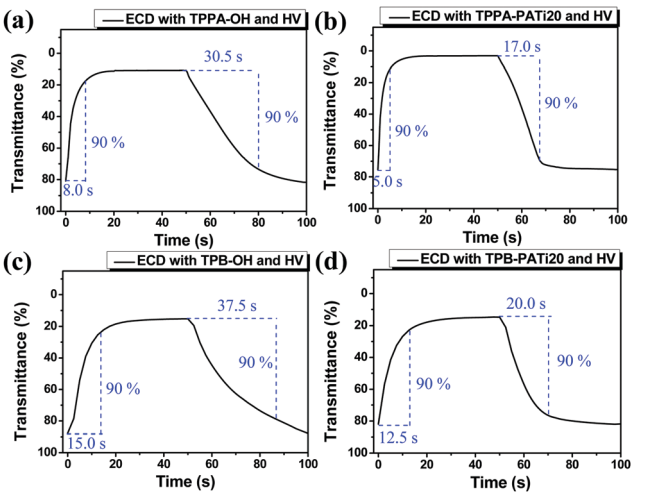

Fig. 5 ECD switching (a) between 1.1 V and −1.15 V for **TPPA-OH** and (b) 1.0 V and −1.05 V for **TPPA-PATi20** at 435 nm; (c) between 1.35 and 1.40 V for **TPB-OH** and (d) 1.25 and −1.3 V for **TPB-PATi20** at 500 nm (thickness: 300 ± 50 nm) on the ITO-coated glass substrate (coated area: 2 cm × 2 cm) in 0.1 M TBABF4/PC electrolyte with 0.015 M HV.

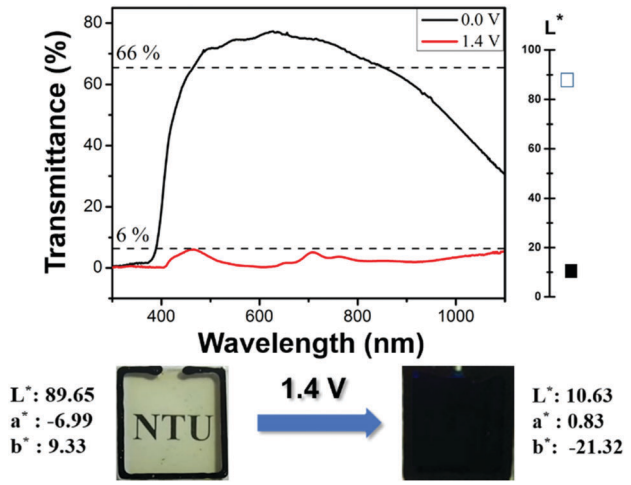

Fig. 6 Transmittance of the ECD derived from the blending of **TPPA-PATi20** and **TPB-PATi20** between 0 V and 1.4 V (air as background), thickness: 900 ± 100 nm on the ITO-coated glass substrate coated area: 2 cm × 2 cm) in 0.1 M $TBABF_4$/PC electrolyte with 0.015 M HV.

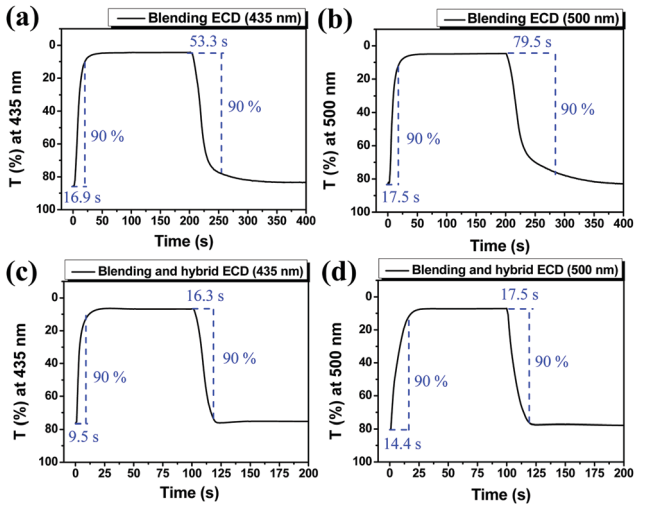

Fig. 7 Electrochromic switching behaviour of (a and b) **TPPA-OH** and **TPB-OH** blended ECD between 1.5 V and −1.6 V, cycle time of 400 s for each cycle; (c and d) **TPPA-PATi20** and **TPB-PATi20** blended hybrid ECD between 1.4 V and −1.5 V (thickness: 900 ± 100 nm on the ITO-coated glass substrate, size: 2 cm × 2 cm) in 0.1 M $TBABF_4$/propylene carbonate electrolyte with 0.015 M HV, and a cycle time of 200 s for each cycle.

by combining the electron acceptors of TiO_2 and HV into the EC devices, a synergetic effect could be observed both in lowering the oxidation potential and enhancing the response capability, especially for the bleaching process. After merging TiO_2/HV into the ECDs, the bleaching time could be significantly reduced to almost half the values of the pristine ones. TiO_2 bonded to the nearby backbone of the PAs plays an important role in temporarily storing electrons released from the anodic EC PAs, and the received electrons remained in the TiO_2 hybrid film adhered on the surface of the anode electrode. Therefore, the electrons could return much faster back to the redox-active triarylamine units of the PAs, resulting in a dramatic enhancement of response capability in the bleaching process compared to just the ambipolar HV system. Consequently, these TiO_2/HV ECDs demonstrate that not only an obvious effect on the reduction of working response time but also long-term electrochemical stability could be achieved simultaneously. Thus, the change of ΔT was only 2% after 300 continuous switching cycles, as shown in Fig. S9 (ESI†). Furthermore, the EC coloration efficiency (η = $\delta OD/Q$) and injected charge (Q) after various switching steps were also monitored and are summarized in Table S6 (ESI†).

Electrochromic behaviors of panchromatic hybrid ECDs

Based on the spectroelectrochemical results we have discussed in the previous section, we can easily prepare ECDs that can switch between the transparent state and a black color state by just combining TPPA-PA, TPB-PA and HV in one system. In order to obtain panchromatic ECDs with a higher response capability during the switching process, the characteristic optical absorption behaviours of **TPPA-PATi20** and **TPB-PATi20** based on spectroelectrochemical measurements were merged together and the blended system was used to prepare the ECDs. According to our previous study, an extremely high optical contrast over the whole visible light region could be attained by using the blended PA film with a thickness of about 1 μm. However, the response capability was greatly sacrificed even though HV was already included in the system. Consequently, the TiO_2/HV system will be very important for ECD applications. As mentioned above, the 1st oxidation potentials of the ECDs were **TPPA-PATi20/HV** (1.0 V) and **TPB-PATi20/HV** (1.25 V), respectively, while the appropriate driving potential needed in the blended hybrid system was 1.4 V to fully switch to the 1st oxidation state ascribed to the film thickness around 900 nm. The transmittance over the whole visible light region was lower than 6% at an applied potential of 1.4 V and ΔL was close to 80, as depicted in Fig. 6, demonstrating that a similar contrast to the previous study could be attained under a lower driving voltage. Furthermore, the colouring and bleaching time based on the characteristic absorption peaks of **TPPA** and **TPB** could also be significantly shortened, as illustrated in Fig. 7. Besides, the switching stability revealed an obvious amelioration during the 40 cycles of testing, as shown in Fig. S10 (ESI†).

Conclusions

Novel redox-active polyamides with a hydroxyl group and their TiO_2 hybrids obtained by the sol–gel reaction have been successfully synthesized for the fabrication of novel ECDs with enhanced electrochemical response capability and stability. TiO_2 in the hybrid system played a crucial role as charge storage units connected to the polymer backbone *via* covalent bonding that could effectively deliver electrons back and forth between the triarylamine moieties and during the oxidation redox process at the anode electrode. Consequently, response time could be substantially reduced both in switching and bleaching procedures. Furthermore, the ECD comprising both HV and TiO_2 exhibited excellent EC performance, especially for bleaching time.

A response time of more than 30 s for the devices based on **TPPA-PA/HV** or **TPB-PA/HV** is necessary for the bleaching process, while with the help of TiO_2, in the cases of **TPPA-PATi20/HV** and **TPB-PATi20/HV**, only half the time of those system containing only HV is needed. These results demonstrate the synergetic effect on the improvement of EC performance. Therefore, the panchromatic ECDs with enhanced response capability could be obtained by integrating **TPPA-PATi20/HV** and **TPB-PATi20/HV**, and they displayed excellent EC performance such as transmittance over the whole visible light region reaching less than 6% with an extremely high ΔL close to 80. Thus, by this facile approach of utilizing redox-active polyamide–TiO_2 hybrids, the most crucial issue of working response time could be effectively improved in addition to long-term electrochemical stability that could be achieved simultaneously.

Conflicts of interest

There are no conflicts to declare.

Acknowledgements

This work was financially supported by the ''Advanced Research Center for Green Materials Science and Technology'' from The Featured Area Research Center Program within the framework of the Higher Education Sprout Project by the Ministry of Education (107L9006) and the Ministry of Science and Technology in Taiwan (MOST 107-3017-F-002-001 and 104-2113-M-002-002-MY3).

Notes and references

1 V. D. Neff, *J. Electrochem. Soc.*, 1978, **125**, 886.
2 (*a*) K. Takada, R. Sakamoto, S.-T. Yi, S. Katagiri, T. Kambe and H. Nishihara, *J. Am. Chem. Soc.*, 2015, **137**, 4681; (*b*) J. T. S. Allan, S. Quaranta, I. I. Ebralidze, J. G. Egan, J. Poisson, N. O. Laschuk, F. Gaspari, E. B. Easton and O. V. Zenkina, *ACS Appl. Mater. Interfaces*, 2017, **9**, 40438; (*c*) P. C. Mondal, V. Singh and M. Zharnikov, *Acc. Chem. Res.*, 2017, **50**, 2128.
3 S. K. Deb, *Appl. Opt.*, 1969, **8**, 192.
4 L. Zhao, L. Zhao, Y. Xu, T. Qiu, L. Zhi and G. Shi, *Electrochim. Acta*, 2009, **55**, 491.
5 R. J. Mortimer and T. S. Varley, *Chem. Mater.*, 2011, **23**, 4077.
6 (*a*) U. Bach, D. Corr, D. Lupo, F. Pichot and M. Ryan, *Adv. Mater.*, 2002, **14**, 845; (*b*) C. Ma, M. Taya and C. Xu, *Polym. Eng. Sci.*, 2008, **48**, 2224; (*c*) S. Beaupré, A.-C. Breton, J. Dumas and M. Leclerc, *Chem. Mater.*, 2009, **21**, 1504.
7 H. J. Yen and G. S. Liou, *Polym. Chem.*, 2018, **9**, 3001.
8 (*a*) H. S. Liu, B. C. Pan, D. C. Huang, Y. R. Kung, C. M. Leu and G. S. Liou, *NPG Asia Mater.*, 2017, **9**, e388; (*b*) D. Weng, Y. Shi, J. Zheng and C. Xu, *Org. Electron.*, 2016, **34**, 139.
9 C. L. Tsai, T. M. Lee and G. S. Liou, *Polym. Chem.*, 2016, **7**, 4873.
10 (*a*) Y. H. Chou, C. L. Tsai, W. C. Chen and G. S. Liou, *Polym. Chem.*, 2014, **5**, 6718; (*b*) T. T. Huang, C. L. Tsai, S. Tateyama, T. Kaneko and G.-S. Liou, *Nanoscale*, 2016, **8**, 12793; (*c*) C. J. Chen, C. L. Tsai and G. S. Liou, *J. Mater. Chem. C*, 2014, **2**, 2842.
11 V. Etacheri, C. Di Valentin, J. Schneider, D. Bahnemann and S. C. Pillai, *J. Photochem. Photobiol., C*, 2015, **25**, 1.
12 V. L. Davis, S. Quaranta, C. Cavallo, A. Latini and F. Gaspari, *Sol. Energy Mater. Sol. Cells*, 2017, **167**, 162.
13 K. Lee, A. Mazare and P. Schmuki, *Chem. Rev.*, 2014, **114**, 9385.
14 (*a*) B. R. Huang, T. C. Lin and Y. M. Liu, *Sol. Energy Mater. Sol. Cells*, 2015, **133**, 32; (*b*) X. Yang, L. Chi, C. Chen, X. Cui and Q. Wang, *Phys. E*, 2015, **66**, 120; (*c*) X. Fu, C. Jia, Z. Wan, X. Weng, J. Xie and L. Deng, *Org. Electron.*, 2014, **15**, 2702; (*d*) Y. Osman, R. Jamal, A. Rahman, F. Xu, A. Ali and T. Abdiryim, *Synth. Met.*, 2013, **179**, 54.
15 S. Xiong, S. L. Phua, B. S. Dunn, J. Ma and X. Lu, *Chem. Mater.*, 2010, **22**, 255.
16 H. J. Yen, K. Y. Lin and G. S. Liou, *J. Mater. Chem.*, 2011, **21**, 6230.
17 H. J. Yen and G. S. Liou, *Chem. Mater.*, 2009, **21**, 4062.
18 Y. Xiao, L. Chu, Y. Sanakis and P. Liu, *J. Am. Chem. Soc.*, 2009, **131**, 9931.
19 Y. Noboru, M. Makoto and H. Fukuji, *J. Polym. Sci., Polym. Chem. Ed.*, 1975, **13**, 1373.

